International Mathematical Forum, Vol. 7, 2012, no. 49, 2431 - 2448

A Lagrangian Method for a Smooth Tomographic Reconstruction of Binary Axially Symmetric Objects

Ali Srour

Lebanese university, Faculty of Science, Section I, Tyre, Lebanon
ali.srour.lb@gmail.com

Abstract

In this paper, we investigate numerically a system of optimality conditions for a smooth minimization problem $(\mathcal{P}_\alpha)$ that arises in tomographic reconstruction of binary axially symmetric objects. We treat the couple (solution, Lagrange multipliers) as a saddle point of the Lagrangian associated to $(\mathcal{P}_\alpha)$, then we use the Uzawa method, and the descent gradient method to give a numerical scheme.

Mathematics Subject Classification: 65K05, 65K15, 65K10

Keywords: Tomographic reconstruction, Variational method, Relaxation, Lagrange multipliers, Mathematical programming method, Lagrangian method

1 Introduction

At present times, the tomographic reconstruction is one of the most effective domains in applied mathematics. The most important strategy that intervenes at this level is the variational method. In [1], I. Abraham, R. Abraham and M. Bergounioux attempt to reconstruct the density of a binary axially symmetric object by using the variational method; with this method, they obtained a non smooth minimization problem $(\mathcal{P})$ with a binary constraint. Because of these difficulties of lack of differentiability and the non-convexity constraint, they cannot apply directly the classical optimization theory to prove the optimality system condition associated to $(\mathcal{P})$. In [6], M. Bergounioux and myself introduced to $(\mathcal{P})$ a few justified modifications from a numerical point of view, we relaxed the binary constraint, and we regularized $(\mathcal{P})$, then we obtained a smooth minimization problem $(\mathcal{P}_\alpha)$ with a non-convexity constraint. Through these modifications, we proved an optimality system associated to$(\mathcal{P}_\alpha)$.

In this paper, we study from a numerical point of view the optimality system obtained in [6]. First, we treat the couple (solution, Lagrange multipliers) as a saddle point of a Lagrangian associated to $(\mathcal{P}_\alpha)$. Second, we

use the Uzawa method and the descent gradient method to establish a stable numerical scheme. This article is structured as follows:

In section 2, we present our model; in section 3, we introduce the problem setting; section 4 is devoted to present the saddle-point formulation; in section 5, we present the numerical scheme; and in section 6, we interpret our numerical results.

2 Presentation of our model

In this article, we are interested in a problem of tomographic reconstruction in order to study the behavior of a material under shock. This technology of tomographic reconstruction consists of reconstructing the volume of a three dimensional object from two dimensional projections; in other words, an object is exposed to a beam of electrons, every point of this object is characterized by its attenuation coefficient. The tomographic method consists of gathering these 2D projections of an X-ray radiography through an object, and from these projections to rebuilding the structure of this object in 3D. These problems were intensively studied since the beginning of 1970's, and it had numerous applications notably in medical imagery (scanner). Using a sufficient number of projections, it is possible to deduct the density in every point of the object (see for instance [8]). In this paper, we are interested in a model proposed by I. Abraham, R. Abraham and M. Bergounioux in [1]. In this model, the authors try to rebuild from a single X-ray radiography the density of a binary object composed of one homogeneous material (drawn in black), and of some holes (in white) (see Fig.1). As this object is noticed under a single radiography, a hypothesis of symmetric is essential to accomplish reconstruction. In [1], the object is assumed to be axially symmetric; with this assumption, it is enough to take a section plane, the **3D** object will be acquired by a rotation around the axis of symmetry. Our work example drawn on Fig.1 represents a symmetric object containing all standard difficulties that may appear such as:

• Several disconnected holes.

• A small holes located on the symmetry axis (where details are expected to be difficult to recover because the noise variance is maximal around the symmetric axis after reconstruction).

• Smaller details on the boundary of the top holes, serving as a test for lower bound detection.

If we assume that u is the density of the initial object, and g is the one of the observed image, the problem of reconstruction is to find u such that $Hu = g$ where H is the projection operator from $L^2(\Omega)$ to $L^2(\Omega)$ given for a symmetric axial object by:

Figure 1: The real object

$$Hu(y,z) = \int_{|y|}^{+\infty} u(r,z) \frac{r}{\sqrt{r^2 - y^2}} dr. \tag{1}$$

Here, Ω is a regular open bounded in $\mathbb{R}^2$ which represents the domain of image ($\Omega = [0,a] \times (-a,a), a > 0$).
A continuity result is established to H from $L^2(\Omega)$ to $L^2(\Omega)$ (see [2] Lemma 1). To find u, it is enough to prove H^{-1}, the inverse operator H^{-1} is given in [2] by:

$$u(r,z) = H^{-1}g(r,z) = -\frac{1}{\pi} \int_r^a \frac{\frac{\partial g}{\partial y}(y,z)}{\sqrt{y^2 - r^2}} dy, \tag{2}$$

for all $(r,z) \in \Omega$.
Because of the derivative term, the operator H^{-1} cannot be extended as a continuous linear operator from $L^p(\Omega)$ to $L^q(\Omega)$ for suitable a p and q. Concretely, this means that a small variation of the measure induces significant errors on the reconstruction, then, the application of H^{-1} provides a deficient and imperfect reconstruction of the original image.

Moreover, due to the experiment step, there is an additional noise perturbation to the given image g. This perturbation assumed to be an addition of Gaussian white noise, denoted τ, of zero mean, and of standard deviation σ_τ. Other perturbations, such as blur due to the detector response, and X-ray source spot size, or blur motion are not taken into account in our study. With these assumptions, the projection of an object u is

$$g = Hu + \tau.$$

The instability of reconstruction using H^{-1} is illustrated in Fig.2. The real object is drawn on Fig.2a, the projection g is drawn on Fig.2b, and the reconstruction using the inverse operator H^{-1} applied to g is drawn on Fig.2c.

(a) the real object u.

(b) the projection g.

(c) Reconstruction $H^{-1}(g)$.

Figure 2: Instability of reconstruction by using H^{-1}.

3 Variational method: The setting problem

As the method of inverse projection is instable, we are going to use the variational method to find the density u. With this method, we search u as the minimum of the following problem

$$(\mathcal{P}) \quad \begin{cases} \min F_o(u) := \dfrac{1}{2}\|Hu - g\|^2_{L^2(\Omega)} + \lambda J(u), \\ u \in \mathcal{D}\ , \end{cases}$$

where

$$\mathcal{D} = \{u \in BV(\Omega) : u(u-1) = 0 \text{ a.e in } \Omega\}\,,$$

where $BV(\Omega)$ denotes the space of the functions of bounded variation space defined by

$$BV(\Omega) = \left\{u \in L^1(\Omega) : J(u) < \infty\right\},$$

with

$$J(u) = \sup\left\{\int_\Omega u(x)\mathrm{div}(\phi(x))dx : \phi \in C^1_c(\Omega, \mathbb{R}^2), \|\phi\|_\infty \leq 1\right\}.$$

Here $C^1_c(\Omega, \mathbb{R}^2)$ denotes the space of the C^1 functions with compact support in Ω with value in $\mathbb{R}^2$.

In the following, we shall denote $||\cdot||$ the $L^2(\Omega)$-norm. In the same way, $(\cdot,\cdot)_2$ denotes the $L^2(\Omega)$- scalar product, $(\cdot,\cdot)_{H^1}$ denotes the $H^1(\Omega)$- scalar product and $\langle\cdot,\cdot\rangle_{V',V}$, the duality product between V' and V, where V is a Banach space and V' is the dual space of V.

Similar problems have been studied by Aubert and Kornprobst in [5], Acar and Vogel in [3], Vogel and Oman in [12] and Casas, Kunisch and Pola [7]. Here, the difficulty comes from the fact that the feasible domain $\mathcal{D}$ is not

convex and its interior is empty for most usual topologies. Plus, the total variation $J(u)$ of a function u in $BV(\Omega)$ is not Frechet differentiable.

In [2], Abraham, Bergounioux and Trelat have also considered the problem $(\mathcal{P})$; they proved the existence of (at least) a solution of $(\mathcal{P})$ in $BV(\Omega)$, and by using the penalization technique to deal with binary constraints, they gave a first order optimality condition. The optimality system they obtained was not suitable for numerical purposes, and they rather solved the penalized system.

In [6], we look for different strategies to study the problem $(\mathcal{P})$ from a numerical point of view. In a first step, and in order to avoid the cost functional lack of differentiability, we consider the problem where the total variation $J(u)$ is replaced by the $L^2(\Omega)$-norm of the gradient of $u \in H^1(\Omega)$. Therefore, the underlying space is not $BV(\Omega)$ but $H^1(\Omega)$.

In a second step, and in order to avoid the difficulty of the domain $\mathcal{D}$, we consider a relaxed formulation, that $0 \leq u \leq 1$, $(u, 1-u)_2 \leq \alpha$, where $\alpha > 0$. The relaxation of the binary constraint is motivated and justified numerically. Indeed, it is not possible to ensure $(u, 1-u)_2 = 0$ during computation but rather $(u, 1-u)_2 \leq \alpha$ where α may chosen small as wanted.

After these modifications, we consider the smooth relaxed problem:

$$(\mathcal{P}_\alpha) \quad \left\{ \begin{array}{l} \min F(u) := \dfrac{1}{2}\|Hu - g\|^2 + \dfrac{\lambda}{2}\|\nabla u\|^2, \\ u \in \mathcal{D}_\alpha \end{array} \right.$$

where $\alpha > 0$ and $\mathcal{D}_\alpha$ is given by:

$$\mathcal{D}_\alpha := \left\{ u \in H^1(\Omega) \mid 0 \leq u \leq 1 \ , \ (u, 1-u)_2 \leq \alpha \ \right\}. \tag{3}$$

In [6], we prove that the problem $(\mathcal{P}_\alpha)$ have at least a solution in $H^1(\Omega)$. But, since the constraint $\mathcal{D}_\alpha$ is also not convex, it is not possible to find the "admissible" directions to compute derivatives. We need a general qualification assumption to derive optimality conditions for that, we are going to use general mathematical programming problems results, and optimal control in Banach spaces (see Zowe and Kurcyusz [9], and Tröltzsch [11, 10]).

To apply the method of mathematical programming to $(\mathcal{P}_\alpha)$, we introduce a virtual control variable, we can write the problem $(\mathcal{P}_\alpha)$ as:

$$(\mathcal{P}_\alpha) \quad \left\{ \begin{array}{l} \min F(u) \\ (u, v) \in \mathcal{C}_\alpha, \end{array} \right.$$

where

$$\mathcal{C}_\alpha := \{(u, v) \in H^1(\Omega) \times L^2(\Omega) \mid u \geq 0, \ v \geq 0, \ u + v = 1 \ \text{ a.e. on } \Omega, \ (u, v)_2 \leq \alpha\} \ . \tag{4}$$

We denote by $(u_\alpha, v_\alpha = 1 - u_\alpha)$ the solution of $(\mathcal{P}_\alpha)$ in $H^1(\Omega) \times L^2(\Omega)$, by using the mathematical programming method and after a step of penalization, we may derive optimality conditions:

Theorem 3.1 Assume u_α is a solution to $(\mathcal{P}_\alpha)$ and $v_\alpha = 1 - u_\alpha$. There exists a Lagrange multiplier $(q_\alpha, r_\alpha) \in \mathcal{M}(\Omega) \times \mathbb{R}^+$ such that:

$$\forall u \in H^1(\Omega) \cap L^\infty(\Omega) \text{ such that } u \geq 0$$
$$(H^*(Hu_\alpha - g) + r_\alpha v_\alpha, u - u_\alpha)_2 + \lambda \left(\nabla u_\alpha, \nabla(u - u_\alpha)\right)_2 + \langle q_\alpha, u - u_\alpha \rangle_{\mathcal{M},L^\infty} \geq 0, \tag{5a}$$

$$\forall v \in \mathcal{V}_{ad} \cap L^\infty(\Omega) \qquad \langle q_\alpha, v - v_\alpha \rangle_{\mathcal{M},L^\infty} + r_\alpha \left(u_\alpha, v - v_\alpha\right)_2 \geq 0, \tag{5b}$$

$$r_\alpha \left[(u_\alpha, v_\alpha)_2 - \alpha\right] = 0, \tag{5c}$$

where

$$\mathcal{V}_{ad} = \left\{ v \in H^1(\Omega) : v \geq 0 \text{ a.e} \right\}.$$

Now, we are interested in the above optimality system to prove a numerical scheme to $(\mathcal{P}_\alpha)$. With this kind of system, we will use a Lagrangian point of view, then we are going to formulate the couple (solution, Lagrangian multipliers) as saddle-point existence result.

4 Saddle-point Formulation

Let L^α be the Lagrangian function associated to problem $(\mathcal{P}_\alpha)$ defined on $H^1(\Omega) \times L^2(\Omega) \times \mathcal{M}(\Omega) \times \mathbb{R}$ by:

$$L^\alpha(u, v, q, r) = \frac{1}{2}||Hu - g||^2 + \frac{\lambda}{2} \|\nabla u\|^2 + \langle q, u + v - 1 \rangle_{\mathcal{M},L^\infty} + r[(u, v)_2 - \alpha]$$

From now, we denote by:

$$F(u) = \frac{1}{2}||Hu - g||^2 + \frac{\lambda}{2} \|\nabla u\|^2 .$$

Theorem 4.1 Let (u_α, v_α) be a solution of $(\mathcal{P}_\alpha)$, then $(u_\alpha, v_\alpha, q_\alpha, r_\alpha)$ satisfies

$$L^\alpha(u_\alpha, v_\alpha, q_\alpha, r_\alpha) \geq L^\alpha(u_\alpha, v_\alpha, q, r) \quad \forall (q, r) \in \mathcal{M} \times \mathbb{R}^+. \tag{6}$$

and

$$\nabla_{u,v} L^\alpha(u_\alpha, v_\alpha, q_\alpha, r_\alpha)(u - u_\alpha, v - v_\alpha) \geq 0, \text{for all } (u, v) \in \mathcal{U}_{ad} \cap L^\infty \times \mathcal{V}_{ad} \cap L^\infty. \tag{7}$$

Proof 4.1 The first assertion comes from the fact that for all $(q, r) \in \mathcal{M} \times \mathbb{R}^+$,

$$L^\alpha(u_\alpha, v_\alpha, q, r) = F(u_\alpha) + r[(u_\alpha, v_\alpha) - \alpha] \leq F(u_\alpha),$$

and

$$F(u_\alpha) = L^\alpha(u_\alpha, v_\alpha, q_\alpha, r_\alpha).$$

Moreover, adding (5a) and (5b), we obtain exactly the second part of theorem 4.1.

We denote by

$$\mathcal{A} = \mathcal{U}_{ad} \cap L^\infty \times \mathcal{V}_{ad} \cap L^\infty \times \mathcal{M} \times \mathbb{R}^+.$$

Because of the bilinear term $(u, v)_2 - \alpha$, the Lagrangian L^α is not convex and the theorem 4.1 is not sufficient to ensure the existence of a saddle point of L^α. But, it is easy to see that this theorem is still valid if we replace L^α by the linearized Lagrangian function $\mathcal{L}^\alpha$:

$$\mathcal{L}^\alpha(u, v, q, r) = F(u) + (q, u + v - 1)_{\mathcal{M}, L^\infty} + r[(u, v_\alpha)_2 + (u_\alpha, v)_2 - 2\alpha].$$

More precisely we have:

Theorem 4.2 The couple $(u_\alpha, v_\alpha, q_\alpha, r_\alpha)$ (solution, Lagrange multiplier) is a saddle point of the linearized Lagrangian function $\mathcal{L}^\alpha$ on $\mathcal{A}$:

$$\mathcal{L}^\alpha(u_\alpha, v_\alpha, q, r) \leq \mathcal{L}^\alpha(u_\alpha, v_\alpha, q_\alpha, r_\alpha) \leq \mathcal{L}^\alpha(u, v, q_\alpha, r_\alpha) \text{ forall } (u, v, q, r) \in \mathcal{A}.$$

Proof 4.2 We get first the left hand part of the above inequality since for any $(q, r) \in \mathcal{M} \in \mathbb{R}^+$

$$\mathcal{L}^\alpha(u_\alpha, v_\alpha, q, r) = F(u_\alpha) + 2r[(u_\alpha, v_\alpha)_2 - \alpha] \leq F(u_\alpha) = \mathcal{L}^\alpha(u_\alpha, v_\alpha, q_\alpha, r_\alpha).$$

The right hand part comes from

$$\nabla_{u,v}\mathcal{L}^\alpha(u_\alpha, v_\alpha, q_\alpha, r_\alpha) = \nabla_{u,v}L^\alpha(u_\alpha, v_\alpha, q_\alpha, r_\alpha),$$

and the convexity of $\mathcal{L}^\alpha$.

In the case, where the bilinear constraint is inactive $(u_\alpha, v_\alpha) < \alpha$ we get $r_\alpha = 0$. In this case it is easy to see that $\nabla_{u,v}\mathcal{L}^\alpha(u_\alpha, v_\alpha, q_\alpha, r_\alpha)$ is then equal that $\nabla_{u,v}L^\alpha(u_\alpha, v_\alpha, q_\alpha, r_\alpha)$ and the above theorem yields:

$$L^\alpha(u_\alpha, v_\alpha, q_\alpha, r_\alpha) \leq L^\alpha(u, v, q_\alpha, r_\alpha),$$

and then $(u_\alpha, v_\alpha, q_\alpha, r_\alpha)$ is a saddle point of L^α on $\mathcal{A}$.

Remark 4.1 As in our initial problem $(\mathcal{P}_\alpha)$, we search for the couple (u_α, v_α) such that $u_\alpha \cdot v_\alpha = u_\alpha(1 - u_\alpha)$ is close to 0, it is therefore interesting to be studying from a numerical point of view the case where the constraint $(u, v)_2$ is inactive i.e:

$$(u, v)_2 < \alpha.$$

5 numerical scheme: Inactive constraint

The basic method to compute a saddle point is the Uzawa algorithm and the descent gradient method [4]. With this method we search the couple (Solution; Lagrangian multiplier) as the following way:

Algorithm ($\mathcal{A}$)

Step 0 Initialization: set $n = 0$, choose $u^0 \in \mathcal{U}_{ad}, q^0 \in L^2(\Omega), v^{-1} \in \mathcal{V}_{ad}$.
Step 1 Compute:

$$u^n = \text{argmin } L^\alpha(u, v^{n-1}, q^n, r^n) \quad \text{sur} \quad \mathcal{U}_{ad}.$$

$$v^n = \text{argmin } L^\alpha(u^n, v, q^n, r^n) \quad \text{sur} \quad \mathcal{V}_{ad}.$$

Step 2 compute q^n:

$$q^{n+1} = q^n + \rho_1(u^n + v^n - 1), \rho_1 \geq 0.$$

Step 3 compute r^n:

$$r^{n+1} = r^n + \rho_2[(u^n, v^n)_2 - \alpha]_+, \rho_2 \geq 0.$$

Step 4 Criterion of stopping : they stop algorithm as soon as $||u^{n+1} - u^n||_\infty < tol$ and $||q^{n+1} - q^n||_\infty < tol$, where tol is a positive real number.

To calculate the first step, we use the gradient descendant method: we search u^n and v^n as following:

$$u^{n+1} = [u^n - \mu_n \nabla_u L^\alpha(u^n, v^n, r^n, q^n)]_+,$$

where

$$\mu_n = \inf_{\mu \in \mathbb{R}} L^\alpha(u^n - \nabla_u L^\alpha, v^n, r^n, q^n).$$

In the some way,

$$v^{n+1} = [v^n - \delta_n \nabla_v L^\alpha(u^n, v^n, r^n, q^n)]_+,$$

where

$$\delta_n = \inf_{\delta \in \mathbb{R}} L^\alpha(u^n, v^n - \nabla_v \mathcal{L}^\alpha, r^n, q^n).$$

In addition, as the study of a measure is too hard from a numerical point of view, we deal in step 2 q_α as a function in $L^2(\Omega)$.

The discretization process is the standard Finite Difference Method. For the projection operator H, we use its explicit formula, we prove the matrix

associated to this operator. The discretized image is represented by a $N \times N$ array identified with a N^2 vector. Due to the symmetry, it suffices to deal with half an image of size $N \times N/2$. In our study, the projected image (observed data) is perturbed with a Gaussian noise τ with standard deviation σ_τ,

$$\tau(x) = \frac{1}{\sqrt{2\pi}\sigma_\tau} e^{-\frac{|x|^2}{2\sigma_\tau^2}}.$$

6 Interpretation of numerical results

The algorithm $(\mathcal{A})$ shows a strong sensitivity with respect to the constant λ, and a weak sensitivity with respect to α. we fix $\alpha = 10^{-2}$ then we study with the sensibility in comparison to λ.

6.1 Sensitivity with respect to λ.

The algorithm $(\mathcal{A})$ is very sensible with respect the constant of regularization λ. With this term, we increase or we decrease the effect of regularization of the term $||\nabla u||_2^2$. More precisely, for λ is small enough, we recover some information on the edge of the image, but we do not succeed in abolishing efficiently the Gaussian noise with the standard deviation σ_τ. But, a important value of λ, leads to a strong regularization and to an important loss of information on the edge of the image. In order to illustrate the strong dependence on λ, we present the evolution of $||u^{n+1} - u^n||_\infty$, and $||q^{n+1} - q^n||_\infty$ for different values of λ.

As a first step, we test the value of $\lambda = 4.10^{-3}$, $\lambda = 10^{-2}$ and $\lambda = 2.10^{-2}$. We obtain for a Gaussian noise with standard deviation σ_τ, the following evolutions of $||u^{n+1} - u^n||_\infty$ and $||q^{n+1} - q^n||_\infty$.

By observing the graphs of the figures (3),(4) and (5), we notice that, for a relatively small value of λ, the number of iterations increases, and the scheme converges with an average value of iterations greater to 100.

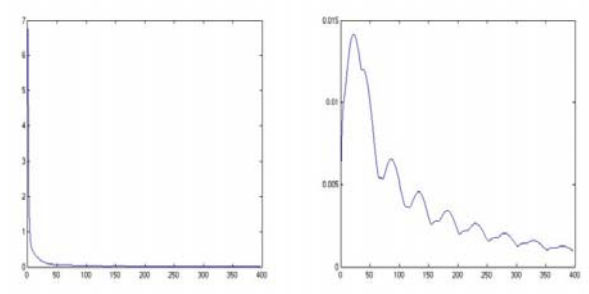

(a) $\lambda = 4.10^{-3}, \alpha = 10^{-2}$.

(b) $\lambda = 4.10^{-3}, \alpha = 10^{-2}$.

Figure 3: Evolution of $||u^{n+1} - u^n||_\infty$ and $||q^{n+1} - q^n||_\infty$ for $\lambda = 0.004$.

We increase the value of λ, we consider $\lambda = 10^{-1}$ and $\lambda = 2.10^{-1}$, with these values of λ, the number of iterations decreases and the algorithm converges faster, then we obtain the graphs in figure 6 and figure (7).

However, if we increase further the value of λ, the algorithm $(\mathcal{A})$ starts to diverge for $tol = 10^{-2}$. Consider for example, the case where $\lambda = 1$, with this value, the evolution of $||u^{n+1} - u^n||_\infty$ and $||q^{n+1} - q^n||_\infty$ is given by the graph in figure 8.

The result shown in the above graphs is confirmed in figure 9 for different values of λ, and with $tol = 10^{-2}$, $\alpha = 10^{-2}$ and $\rho_1 = \rho_2 = 10^{-1}$.

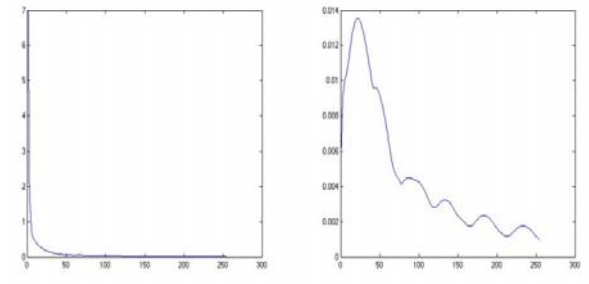

(a) $\lambda = 10^{-2}, \alpha = 10^{-2}$.

(b) $\lambda = 10^{-2}, \alpha = 10^{-2}$.

Figure 4: Evolution of $||u^{n+1} - u^n||_\infty$ and $||q^{n+1} - q^n||_\infty$ for $\lambda = 2.10^{-2}$.

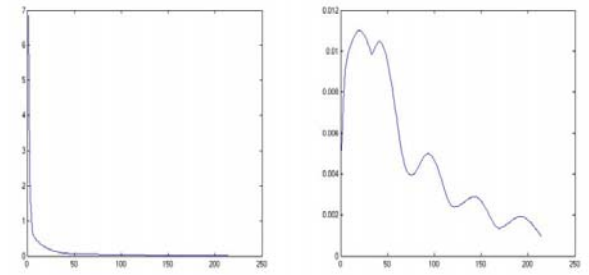

(a) $\lambda = 2.10^{-2}$.

(b) $\lambda = 2.10^{-2}, \alpha = 10^{-2}$.

Figure 5: Evolution of $||u^{n+1} - u^n||_\infty$ and $||q^{n+1} - q^n||_\infty$ for $\lambda = 2.10^{-2}$.

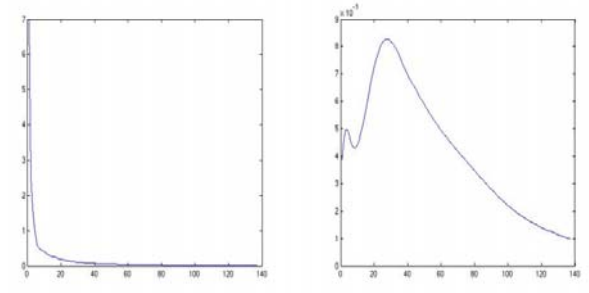

(a) $\lambda = 10^{-1}, \alpha = 10^{-2}$. (b) $\lambda = 10^{-1}, \alpha = 10^{-2}$.

Figure 6: Evolution of $||u^{n+1} - u^n||_\infty$ and $||q^{n+1} - q^n||_\infty$ for $\lambda = 10^{-1}$.

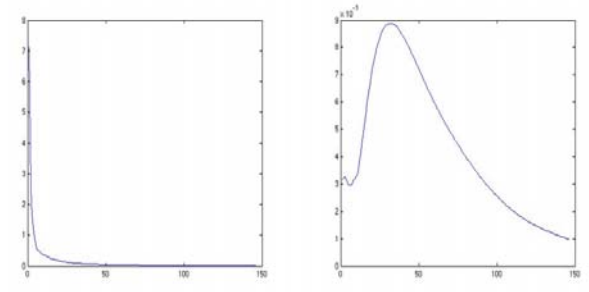

(a) $\lambda = 2.10^{-1}$. (b) $\lambda = 2.10^{-1}$.

Figure 7: Evolution of $||u^{n+1} - u^n||_\infty$ and $||q^{n+1} - q^n||_\infty$ for $\lambda = 2.10^{-1}$.

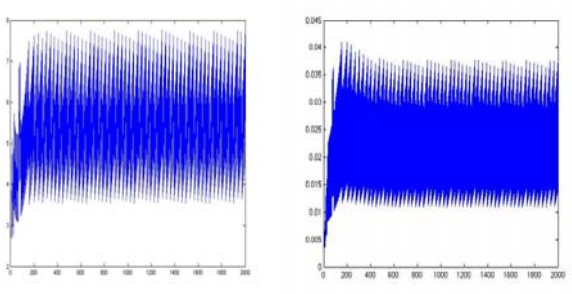

(a) $\lambda = 1, \alpha = 10^{-2}$. (b) $\lambda = 1, \alpha = 2.10^{-1}$.

Figure 8: Evolution of $||u^{n+1} - u^n||_\infty$ and $||q^{n+1} - q^n||_\infty$ for $\lambda = 1$ and 2000 iterations .

λ	iterations	$\|\|u^{n+1} - u^n\|\|_\infty$	F	time(s)
5e-03	2e+03	2e-04	12734+03	153
1e-02	1575	9.7888-05	1.0131e+03	112
2e-02	933	9.9491e-05	744.8284	87
5e-02	792	9.9775e-05	534. 2125	49
6e-02	540	9.9978e-05	448.8426	57
1e-01	605	9.9393e-05	374. 0889	47
2e-01	473	9.9923e-05	334.6922	37
1e-00	2000	1.4574	216.4331	160

Table 1: Sensibility with respect to λ, $tol = 10^{-4}$ and $it_{max} = 2000$.

Considering $tol = 10^{-4}$, limiting the number of iterations to 2000, we obtain for $\alpha = 10^{-2}, \rho_1 = \rho_2 = 10^{-1}$, as shown in table (1). these results confirm the high sensitivity of the scheme compared to λ. First, the maximum number of iterations is reached in the case where λ is big enough or small enough ($\lambda = 1$ or $\lambda = 4.10^{-3}$), while the scheme converges faster for $\lambda = 10^{-1}$. This same idea is illustrated by the value of $||u^{n+1} - u^n||_\infty$, the value of the functional F, and the time of execution which is generally short.

By observing the figure 10, we notice that for relatively small value of λ ($\lambda = 5.10^{-3}, \lambda = 2.10^{-2}$), we get some information on the edge of the image but the Gaussian noise is difficult to remove. By increasing the value of λ($\lambda = 10^{-1}, \lambda = 1$), we remove the Gaussian noise but we regularize the edge of the image too much.

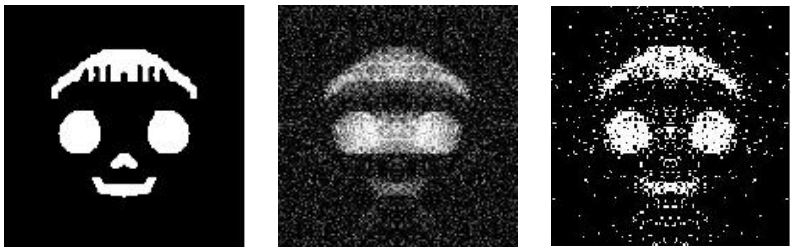

(a) real object. (b) observed image g. (c) $\lambda = 10^{-3}$.

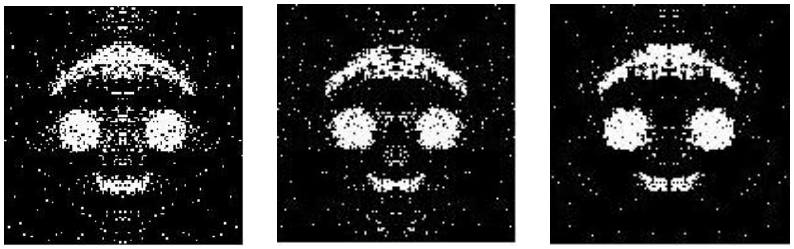

(d) $\lambda = 4.10^{-3}$ (e) $\lambda = 10^{-2}$. (f) $\lambda = 2.10^{-2}$

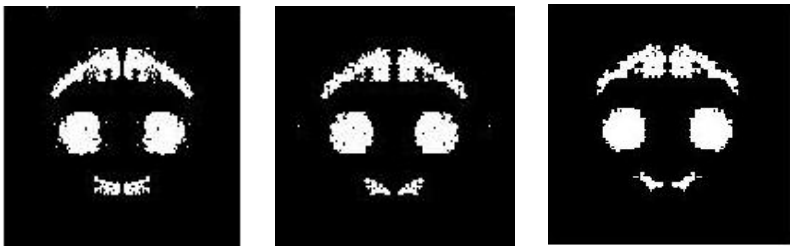

(g) $\lambda = 5.10^{-2}$ (h) $\lambda = 6.10^{-2}$ (i) $\lambda = 10^{-1}$

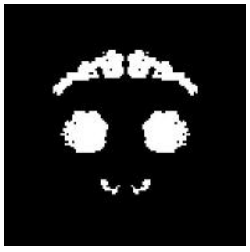

(j) $\lambda = 2.10^{-1}$

Figure 9: Reconstruction for different values of λ.

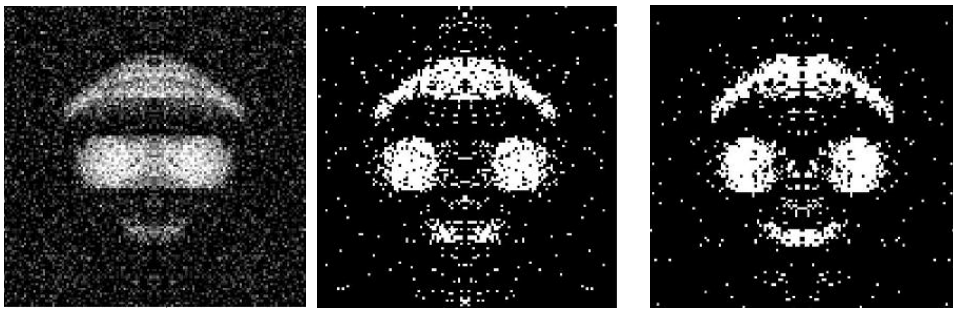

(a) Observed image g. (b) $\lambda = 5.10^{-3}$. (c) $\lambda = 10^{-2}$

(d) $\lambda = 2.10^{-2}$. (e) $\lambda = 5.10^{-2}$ (f) $\lambda = 6.10^{-2}$

(g) $\lambda = 10^{-1}$ (h) $\lambda = 2.10^{-1}$ (i) $\lambda = 1$

Figure 10: Reconstruction for different values of λ with $tol = 10^{-4}$ and $it_{max} = 2000$.

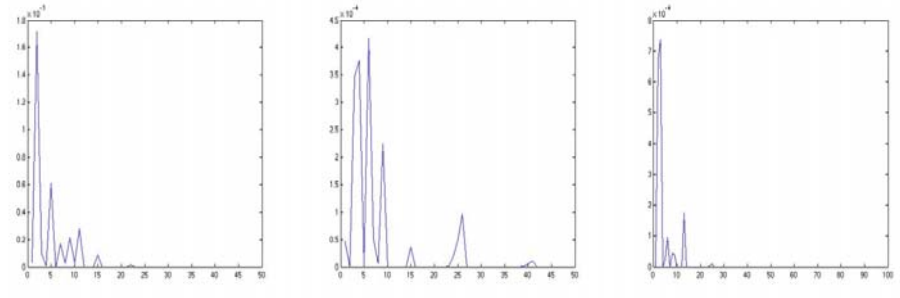

(a) $\alpha = 10^{-3}, \lambda = 10^{-3}$. (b) $\alpha = 10^{-2}, \lambda = 10^{-2}$. (c) $\alpha = 10^{-1}, \lambda = 10^{-2}$.

Figure 11: decrease of $(u, v)_2$ to 0.

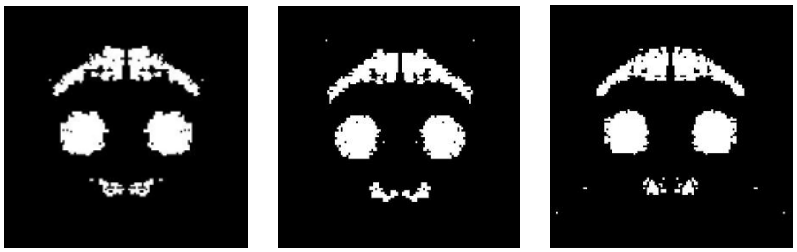

(a) $\alpha = 5.10^{-3}$. (b) $\alpha = 2.10^{-2}$ (c) $\alpha = 10^{-1}$.

Figure 12: Weak dependence with respect to α.

6.2 Sensibility compared to α.

The algorithm $(\mathcal{A})$ has a low sensibility with respect to the parameter α. This weak dependence is due to the fact that the integral $(u, v)_2$ converges rapidly to zero, and by consequence, the inactive assumption $(u, v)_2 < \alpha$ is always verified from a small number of iterations (figure 11). The table 2, and the figure 12 confirm the weak dependence of the scheme compared to α.

7 Conclusion.

The tomographic reconstruction using the algorithm $(\mathcal{A})$ shows a high efficacity compared to the Gaussian noise and the blur introduced by the projection operator H. For certain values of λ ($\lambda = 6.10^{-2}, \lambda = 2.10^{-2}$), we can remove the noise with a relatively short time t, and we obtain some information on the

α	iterations	$\|\|u^{n+1}-u^n\|\|_\infty$	F	time(s)
5e-03	769	9.9088e-05	489.0477	38
1e-02	593	9.9382e-05	462.3171	45
2e-02	516	9.8741e-05	473.16	40
5e-02	792	9.9775e-05	534. 2125	49
1e-01	662	9.9832e-05	442.5995	47

Table 2: Sensibility with respect to α, $tol = 10^{-4}$ and $\lambda = 6.10^{-2}$.

edge of the image. Moreover, as the term $||\nabla u||^2_{L^2}$ highly regulates the edge of the image, an important value of λ ($\lambda = 10^{-1}, \lambda = 5.10^{-1}, \lambda = 1$) leads to a smooth image. There remains a note that, as the points around the axis of symmetry have less information then the point further apart(the concentration of the noise is maximum around the axis of symmetry) a difficulty arising during the reconstruction of these points.

ACKNOWLEDGEMENTS. The author would like to thank Guy Barles and Olivier Ley for their great help, their support, their enriching discussions and their many fruitful suggestions in the preparation of this article. I also would like to express my great fullness to Romain Abraham and Maitine Bergounioux for introducing me to the tomography reconstruction and the studied model. This work was supported by grants of the center region and the national center of scientific research CNRS.

References

[1] I. Abraham, R. Abraham, and M. Bergounioux. An active curve approach for tomographic reconstruction of binary radially symmetric objects. *Numerical Mathematics and advanced Application, Kinisch K, of G, Steinbach, O(Ed), pp 663-670,2008 Springe.*

[2] R. Abraham, M. Bergounioux, and E. Trelat. A penalization approach for tomographic reconstruction of binary axially symmetric objects.

[3] R. Acar and C. R. Vogel. Analysis of bounded variation penalty methods for ill-posed problems. *Inverse Problems*, 10(6):1217–1229, 1994.

[4] G. Allaire. Analyse numerique et optimisation. *Les editions de l'ecole polytechnique*, 2005.

[5] G. Aubert and P. Kornprobst. *Mathematical problems in image processing*, volume 147 of *Applied Mathematical Sciences*. Springer, New York, second edition, 2006. Partial differential equations and the calculus of variations,.

[6] M. Bergounioux and A. Srour. A relaxation method for smooth tomographic reconstruction of binary axially symmetric objects. *Pacific Journal of Optimisation*.

[7] E. Casas, K. Kunisch, and C. Pola. Regularization by functions of bounded variation and applications to image enhancement. *Appl. Math. Optim.*, 40(2):229–257, 1999.

[8] Gabor T. Herman. *Image reconstruction from projections*. Academic Press Inc. [Harcourt Brace Jovanovich Publishers], New York, 1980. The fundamentals of computerized tomography, Computer Science and Applied Mathematics.

[9] J. Zowe S. Kurcyusz. Regularity and stability for the mathematical programming problem in banach spaces. *Applied mathematics and Optimization*, 42, pp.49-62(5), 1979.

[10] F. Tröltzsch. A modification of the zowe and kurcyusz regularity condition with application to the optimal control of noether operator equations with constraints on the control and the state. *Math. Operationforsch. Statist., Ser. Optimization*, 14,.

[11] F. Tröltzsch. Optimality conditions for parabolic control problems and applications. *Teubner Texte, Leipzig,*, (1984).

[12] C. R. Vogel and M. E. Oman. Iterative methods for total variation denoising. *SIAM J. Sci. Comput.*, 17(1):227–238, 1996. Special issue on iterative methods in numerical linear algebra (Breckenridge, CO, 1994).

Received: April, 2012